All-dielectric reflective half-wave plate metasurface based on the anisotropic excitation of electric and magnetic dipole resonances

Hanham, Stephen

DOI:
10.1364/OL.43.000911

All-dielectric reflective half-wave plate metasurface based on the anisotropic excitation of electric and magnetic dipole resonances

Zhijie Ma[1,2,3,4], **Stephen M. Hanham**[5], **Yandong Gong**[4,6], and **Minghui Hong**[2,*]

[1] *NUS Graduate School for Integrative Sciences & Engineering (NGS), National University of Singapore, 117456, Singapore*
[2] *Department of Electrical and Computer Engineering, National University of Singapore, 117576, Singapore*
[3] *Department of Physics, Imperial College London, London SW7 2AZ, UK*
[4] *Institute for Infocomm Research, A*STAR, 138632, Singapore*
[5] *Department of Electronic, Electrical and Systems Engineering, University of Birmingham, Birmingham B15 2TT, UK*
[6] *Institute for Lightwave Technology, Beijing Jiaotong University, Beijing, 100044, China*
[*] *Corresponding author: elehmh@nus.edu.sg*

Compiled January 18, 2018

We present an all-dielectric metasurface that simultaneously supports electric and magnetic dipole resonances for orthogonal polarizations. At resonances, the metasurface reflects the incident light with nearly perfect efficiency and provides a phase difference of π in the two axes, making a low-loss half-wave plate in reflection mode. The polarization handedness of the incident circularly polarized light is preserved after reflection, which is different from either a pure electric mirror or magnetic mirror. With the features of high reflection and circular polarization conservation, the meta-mirror is an ideal platform for the geometric phase-based gradient metasurface functioning in reflection mode. Anomalous reflection with the planar meta-mirror is demonstrated as a proof of concept. The proposed meta-mirror can be a good alternative to plasmonic metasurfaces for future compact and high efficiency meta-devices for polarization and phase manipulation in reflection mode.

OCIS codes: *(160.3918) Metamaterials; (290.0290) Scattering; (260.5430) Polarization; (260.5740) Resonance.*

http://dx.doi.org/10.1364/ao.XX.XXXXXX

Mirrors have a long history and play an important role in modern optical systems. Conventional mirrors are made of metals or contrasting dielectric layers which reflect light with high efficiency. The boundary condition requires the electric field of the reflected wave to have a sudden phase shift of π with respect to the incident wave at the interface of these mirrors, while the magnetic field component experiences no such phase change. With the emergence of metamaterials which obtain their intriguing properties from subwavelength structures, magnetic mirrors with the opposite behaviour have been realized [1–4], that is, the electric field of the reflected waves has zero phase shift while the magnetic field experiences an abrupt π phase change. The characteristics of mirrors made of perfect electrical conductor (PEC) and perfect magnetic conductor (PMC) are illustrated in Fig. 1, respectively. In both situations, when a circularly polarized (CP) light is incident on either a pure electric or magnetic mirror, the reversal of the wavevector direction will lead to the conversion of the handedness of the CP waves, i.e. a left circularly polarized (LCP) incident light will be reflected into a right circularly polarized (RCP) light, and vice versa.

To preserve the polarization helicity of light after reflection, the mirror should exhibit equal reflection amplitudes and the phase relationship $\Delta\varphi = \varphi_x - \varphi_y = \pi$ for the two orthogonal linear polarizations, which is effectively a half-wave plate (HWP) in reflection mode. Conventional methods to manipulate polarization rely heavily on the use of anisotropic materials, which are bulky and not integratable with compact on-chip nano-photonic devices. With metamaterials, the polarization state of light can be engineered almost freely with deeply subwavelength thickness. A wide range of ultra-thin polarization manipulating metasurfaces such as linear or circular polarizers, and wave-plates [5, 6], have been experimentally demonstrated. The reflective HWPs have also been achieved through different designs [7–10]. However, all these designs consist of multi-layer metallic structures or have a metal backplane. In the visible and near-infrared band, the severe losses in plasmonic structures greatly reduces the efficiency of the devices.

Dielectric metasurfaces have been proven to be a promising alternative to the plasmonic counterparts with the advantages of low loss, reduced design and fabrication complexity, and compatibility with the semiconductor industry [11]. Complete polarization and phase controls have been demonstrated with dielectric metasurfaces composed of high aspect ratio silicon

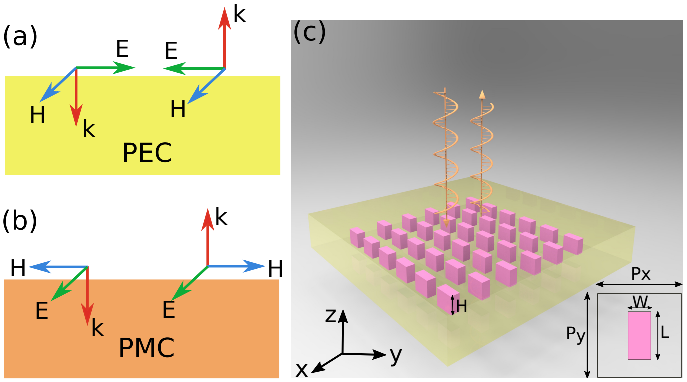

Fig. 1. Illustration of the reflection characteristics of an (a) electric mirror and (b) a magnetic mirror. (c) Schematic of the helicity-preserving meta-mirror, with periodicity $Px = Py =$ 650 nm, resonator width W = 180 nm, resonator length L =370 nm, and height H = 330 nm.

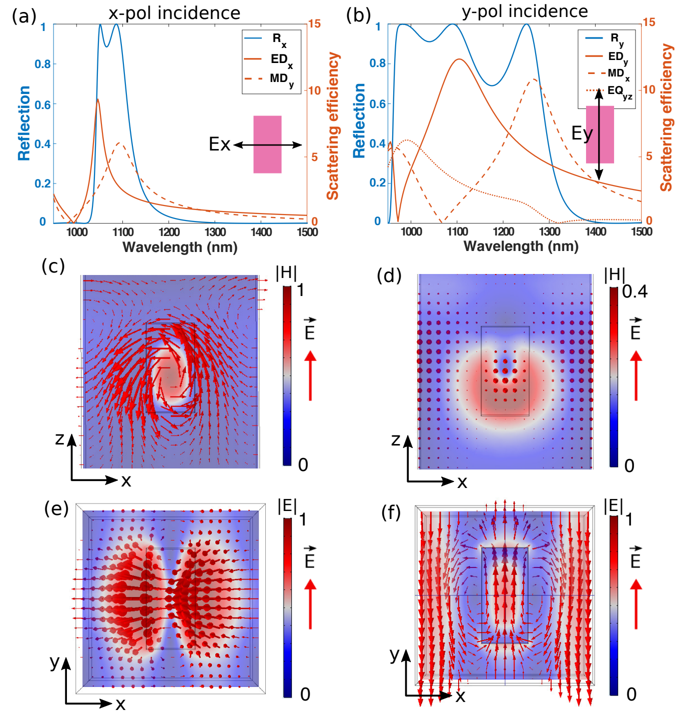

Fig. 2. Reflection spectrum and the multipole coefficients for the (a) x-polarization and (b) y-polarization incidences. (c, d) The magnetic field distribution and electric field vectors in the xz-plane at λ=1090 nm for x-polarization and y-polarization. (e, f) The electric field distribution and electric field vectors in the xy-plane at λ=1090 nm for x- and y-polarization incidences.

nanopillars [12, 13]. More specifically, dielectric-based high-efficiency HWP metasurfaces with gradual varying phases have been achieved in transmission mode for different applications [14–16]. Although these transmissive devices based on high-contrast grating (HCG) can be potentially altered to operate in the reflection mode by properly changing the height of the resonator [17–19], to the best of our knowledge, an all-dielectric HWP in reflection mode has not been manifested yet, the closest is the dielectric HWP reflect-array that nonetheless relies on the metal back plane [20].

In this Letter, we numerically demonstrate an all-dielectric reflective HWP metasurface with high efficiency and phase tuning capability. The meta-mirror consists of arrays of anisotropic subwavelength dielectric resonators in which electric and magnetic dipole resonances are simultaneously excited by the orthogonal linear polarization components of incident wave. Consequently, the meta-mirror exhibits the property of an efficient electric mirror for one linear polarization while behaving like a magnetic mirror for the orthogonal polarization. In addition, with this high reflection and circular polarization conserving characteristics, the meta-mirror is a good platform for geometric phase-based gradient metasurface. We demonstrate that, by changing the orientation of the resonator, different phases of the circularly polarized light with high reflectance can be obtained.

The schematic of the meta-mirror is shown in Fig. 1(c), with the geometry parameters denoted in the inset figure. The structure consists of periodic arrays of silicon cuboid resonators embedded in SiO_2. Such structures can be fabricated by photolithography on silicon-on-insulator wafers followed by reactive-ion etching and the covering of spin-on glass [21]. In our work, finite element method (FEM) in COMSOL Multiphysics was employed for the numerical simulations. In simulation, the environment refractive index is set to be constant as n_0=1.45, and silicon has a relatively constant refractive index of 3.5 in the interested near-infrared region; periodic boundary condition was set in the x and y-directions, and plane waves are normally incident on the structure.

In dielectric metasurfaces, when either an electric or magnetic dipolar mode is excited, the metasurfaces reflect the incident waves with a high efficiency, due to the destructive interference between the incidence and the scattered wave by the resonator in the forward direction [21]. It has been well-proven that [2, 3, 22], at the excitation of electric dipole resonance, the dielectric metasurface can be considered as a material with effectively negative permittivity (ε<0), and it functions as a perfect electric conductor that imposes a sudden phase change of π on the tangential electric field at the reflecting interface while maintaining the direction of the magnetic field. On the other hand, when the magnetic dipole mode is excited, the dielectric metasurface is effectively a magnetic conductor with a negative permeability (μ<0), as a result, the magnetic filed acquires the π phase shift after reflection while the electric field experiences zero phase change. In isotropic dielectric resonators such as a cube or cylinder, the electric and magnetic dipolar modes are usually spectrally well-separated [22]. It was previously demonstrated that the electric and magnetic dipole resonances have different dependences on the dimensions of the resonators so that the two modes can be tuned individually to a certain degree [1, 23], and the periodicities also plays an important role in the spectral position of the modes [24].

To realize the hybrid meta-mirror we propose, the electric and magnetic dipole resonances need to be tailored to overlap in frequency for the orthogonal linear polarizations. This condition was met by finely tuning the geometry parameters of the resonators and the periodicities. The optimized geometry parameters are W = 180 nm, L = 370 nm, H = 330 nm, and the periodicities in x and y directions are $P_x = P_y$ = 650 nm. In Fig. 2(a) and 2(b), the reflection spectra for x and y linear polarizations are plotted (see the blue solid lines), with each peak corresponding to a particular resonance. Owing to the negligibly low loss of silicon in the near-infrared region, the re-

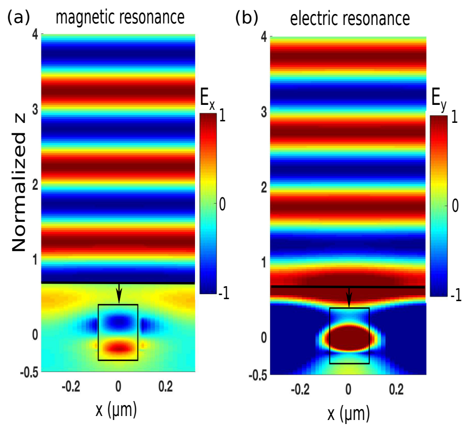

Fig. 3. Snapshots of the E-field of reflected waves under (a) x-pol and (b) y-pol incidences. The z axis is normalized to the effective wavelength λ/n_0, where n_0=1.45 is the environment index and λ=1090 nm. The position of the source is indicated with the solid black line, the solid line box depicts the boundaries of the resonator.

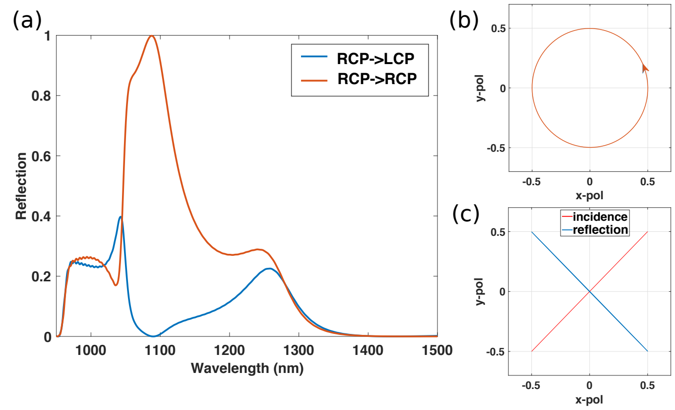

Fig. 4. (a) The reflection spectrum under RCP incidence decomposed into LCP and RCP components. (b) The polarization ellipse at 1090 nm. (c) The polarization ellipses for the incident and reflected lights with 45 degree linear polarization incidence.

flection efficiency can reach nearly 100% at each resonance peak. At non-resonant frequencies, the metasurface is transparent, allowing non-interacting waves to pass with high transmittance, distinguishing itself from metallic meta-mirrors that employ a metal ground plane [20]. With the sub-wavelength periodicity, higher order diffractions are avoided. It can be observed in Fig. 2(a) and 2(b) that at $\lambda = 1090$ nm, the reflection peak for the x-polarization spectrally coincide with that for y-polarization.

To identify the involved resonance modes for a clearer description of the dielectric metasurface, a multipole decomposition method suitable for periodic structures based on the induced current in the resonator was employed [25]. The normalized scattering efficiencies for each Mie resonance mode are plotted in the same figures as reflection spectra for x- and y-polarizations, with the y-axis on the right of the figures. For clarity, only the dominant contributing modes are plotted. In Fig. 2(a), it shows that for x polarized incidence, the peak at $\lambda = 1090$ nm corresponds to a magnetic dipole mode (MD_y) oriented in y-direction, and an electric dipole (ED_x) in x-direction is excited at 1045 nm. For y-polarized incidence, as shown in Fig. 2(b), with electric field along the long axis of the resonator, the two peaks are wider and further separated, the magnetic dipole mode MD_x is excited at a longer wavelength λ=1270 nm, and the electric dipole ED_y coincides with the magnetic dipole of x-pol at 1100 nm. For y-polarized light, at the shorter wavelength λ=980 nm, the electric quadrupole mode (EQ_{yz}) can also be excited in the scatterer, however it does not make significant contribution to the function of the meta-mirror so we do not discuss it further. It should be noted that in our meta-mirror, the peaks of the reflection spectra and the multipole scattering coefficients do not overlap exactly, the slight mismatch is because of the close proximity of the multipole modes and their interference can shift the spectral position of the reflection peaks.

In Fig. 2(c) to 2(f), the near-field distributions are plotted to corroborate the excitation of these modes and to show their characteristics. With the height of the dielectric resonator ($H = 330$ nm) close to the effective wavelength of the incident light in the resonator (λ/n), the excited circular displacement currents inside the resonator forms a magnetic field maxima at the center, oriented in the direction of the incident magnetic field, as shown in Fig. 2(c), which is a feature of the magnetic dipole mode. Fig. 2(e) shows the feature of this mode from the xy-plane. In contrast, under y-polarization incidence, the magnetic response are barely excited, as can been in Fig. 2(d). And in Fig. 2(f), the electric field shows the feature of an electric dipole oriented in the y-direction, with the electric vector inside the resonator pointing in the opposite direction to the incident field. In Fig. 3, the E-field of the reflected waves with x and y-polarization incidences at 1090 nm are plotted, from which it can be observed that at the same distance away from the surface, a phase difference of π exists for the two linear polarizations.

As shown above, at the resonance frequency, the anisotropic meta-mirror reflects the x and y-polarized lights with near-unity efficiency and a phase retardation of π, therefore, the device can be described by the Jones matrix:

$$\hat{r} = \begin{bmatrix} r_{xx} & r_{xy} \\ r_{yx} & r_{yy} \end{bmatrix} = \begin{bmatrix} 1 & 0 \\ 0 & -1 \end{bmatrix} \tag{1}$$

The cross-polarization conversion coeffcients r_{xy} and r_{yx} are zero because of the mirror symmetry of the structure. The reflection spectrum under RCP incidence is decomposed into the two circular polarization as shown in Fig. 4(a). The co-polarized component shows a peak of R=1 at $\lambda = 1090$ nm, suggesting that all the incident RCP light is reflected to the light of the same handedness at resonances. In Fig. 4(b), the polarization ellipse of the reflected wave is plotted for λ =1090 nm, which shows an almost perfect circular polarization state of the same helicity. Fig. 4(c) depicts the polarization ellipses of a 45 degree linearly polarized light and the reflected light of -45 degree linear polarization. The HWP meta-mirror has the disadvantages of a limited bandwidth, which might be improved by engineering the multipole interference judiciously, as demonstrated in the dielectric transmission HWP metasurface [15]. In addition, the optical and electrical properties of silicon can be tuned by photo-induced carrier generation, enabling the active control of the device [26–28].

Lastly, we demonstrate that the meta-mirror can be used for gradient phase control. Geometric phase (also known as Pancharatnam-Berry phase) manipulation is a robust method

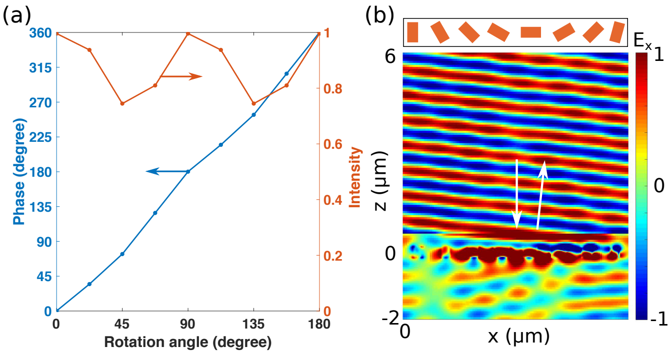

Fig. 5. (a) The intensity and phase of the reflected light of the same circular polarization for arrays of resonators of different orientation angles. (b) The snapshot of the E_x field showing the tilted reflection wavefront.

to control the phase of CP light by simply changing the orientation of the element. In transmission mode, it requires the desired circular component to have the opposite CP state to the incidence light, therefore, elements that operate as HWP is highly desirable to maximize the conversion efficiency, which has been successfully demonstrated with the planar metalens in the visible range [16]. Here, we test the same principle with all-dielectric metasurface operating in the reflection mode. Due to the reversal of the wavevector, for reflection, the geometric phase is acquired by the light of the same CP. In our proposed HWP meta-mirror, ideally, when the dielectric resonator is rotated by an angle θ, the reflected wave of the same handedness is imposed of a phase of 2θ. In Fig. 5(a), the intensity and phase of the reflected waves are plotted for periodic arrays of resonators of different orientations, we can see that a high reflectance can be maintained with a linear phase increase from 0 to 360° with a 45° increment. However, due to the mutual coupling with other resonators, the reflection intensities are lowered at certain angles, and the phases are also slightly deviated from the strict geometric phase of 2θ. These deviations can be possibly compensated by fine tuning of each resonators. As a proof of concept, the eight unit resonators are aligned with the rotation angle θ increasing from 0 to 167.5° linearly, with a increment of 22.5° as shown on top of Fig. 5(b). With CP normal incidence, the reflected wave is tilted with a designed angle. In Fig. 5(b), the snapshot of the E_x field is plotted at λ=1090 nm, showing an anomalous reflection angle $\sim 8°$, agreeing with the theoretical value, and the deflection efficiency into the desired order is 0.73. With less blocks in a supercell and thus a shorter period, the deflection angle can be further increased, although the deflection efficiency will be slightly reduced.

In conclusion, we numerically demonstrated an all-dielectric half-wave plate meta-mirror that derives its function from the anisotropic excitation of the electric and magnetic dipole resonances for orthogonal polarizations. Near-unity reflection amplitude are achieved in the near-infrared region. At resonances, the meta-mirror reflects circularly polarized lights keeping their original handedness, which is a unique property not typically available in conventional mirrors or a purely magnetic mirror metasurface. A multipole analysis of the dielectric resonator was applied for the description of the meta-mirror. We further demonstrated that the HWP meta-mirror is a good platform for the geometric phase-based metasurfaces in reflection mode, with its advantage of high circular polarization conservation. We believe this low-loss design can be a promising alternative to plasmonic polarization transformers and useful for the development of high-efficiency integrable functional metasurfaces.

1. FUNDING

A*STAR, SERC 2014 Public Sector Research Funding (PSF) Grant (SERC Project No.1421200080). The Singapore Economic Development Board (EDB) (No.S15-1322-IAF OSTIn-SIAG).

REFERENCES

1. P. Moitra, B. a. Slovick, Z. Gang Yu, S. Krishnamurthy, and J. Valentine, Appl. Phys. Lett. **104**, 171102 (2014).
2. S. Liu, M. B. Sinclair, T. S. Mahony, Y. C. Jun, S. Campione, J. Ginn, D. A. Bender, J. R. Wendt, J. F. Ihlefeld, P. G. Clem, J. B. Wright, and I. Brener, Optica **1**, 250 (2014).
3. P. Moitra, B. A. Slovick, W. Li, I. I. Kravchencko, D. P. Briggs, S. Krishnamurthy, and J. Valentine, ACS Photonics **2**, 692 (2015).
4. Z. Ma, S. M. Hanham, P. Albella, B. Ng, H. T. Lu, Y. Gong, S. A. Maier, and M. Hong, ACS Photonics **3**, 1010 (2016).
5. N. K. Grady, J. E. Heyes, D. R. Chowdhury, Y. Zeng, M. T. Reiten, A. K. Azad, A. J. Taylor, D. A. R. Dalvit, and H.-T. Chen, Science **340**, 1304 (2013).
6. Y. Ye and S. He, Appl. Phys. Lett. **96**, 1 (2010).
7. J. Hao, Y. Yuan, L. Ran, T. Jiang, J. A. Kong, C. T. Chan, and L. Zhou, Phys. Rev. Lett. **99**, 1 (2007).
8. A. Pors, M. G. Nielsen, G. D. Valle, M. Willatzen, O. Albrektsen, and S. I. Bozhevolnyi, Opt. Lett. **36**, 1626 (2011).
9. M. Pu, P. Chen, Y. Wang, Z. Zhao, C. Huang, C. Wang, X. Ma, and X. Luo, Appl. Phys. Lett. **102** (2013).
10. S. Xiao, H. Mühlenbernd, G. Li, M. Kenney, F. Liu, T. Zentgraf, S. Zhang, and J. Li, Adv. Opt. Mater. **4**, 654 (2016).
11. Q. Zhao, J. Zhou, F. Zhang, and D. Lippens, Mater. Today **12**, 60 (2009).
12. A. Arbabi, Y. Horie, M. Bagheri, and A. Faraon, Nat. Nanotechnol. **10**, 937 (2014).
13. A. Arbabi, Y. Horie, A. J. Ball, M. Bagheri, and A. Faraon, Nat. Commun. **6**, 7069 (2014).
14. M. P. Backlund, A. Arbabi, P. N. Petrov, E. Arbabi, S. Saurabh, A. Faraon, and W. E. Moerner, Nat. Photonics **10**, 459 (2016).
15. S. Kruk, B. Hopkins, I. I. Kravchenko, A. Miroshnichenko, D. N. Neshev, and Y. S. Kivshar, APL Photonics **1**, 030801 (2016).
16. M. Khorasaninejad, W. T. Chen, R. C. Devlin, J. Oh, A. Y. Zhu, and F. Capasso, Science **352**, 1190 (2016).
17. R. Magnusson and M. Shokooh-Saremi, Opt. Express **16**, 3456 (2008).
18. F. Lu, F. G. Sedgwick, V. Karagodsky, C. Chase, and C. J. Chang-Hasnain, Opt. Express **18**, 12606 (2010).
19. C. J. Chang-Hasnain and W. Yang, Adv. Opt. Photonics **4**, 379 (2012).
20. Y. Yang, W. Wang, P. Moitra, I. I. Kravchenko, D. P. Briggs, and J. Valentine, Nano Lett. **14**, 1394 (2014).
21. M. Decker, I. Staude, M. Falkner, J. Dominguez, D. N. Neshev, I. Brener, T. Pertsch, and Y. S. Kivshar, Adv. Opt. Mater. **3**, 813 (2015).
22. J. C. Ginn, I. Brener, D. W. Peters, J. R. Wendt, J. O. Stevens, P. F. Hines, L. I. Basilio, L. K. Warne, J. F. Ihlefeld, P. G. Clem, and M. B. Sinclair, Phys. Rev. Lett. **108**, 097402 (2012).
23. I. Staude, A. E. Miroshnichenko, M. Decker, N. T. Fofang, S. Liu, E. Gonzales, J. Dominguez, T. S. Luk, D. N. Neshev, and I. Brener, ACS Nano **7**, 7824 (2013).
24. K. E. Chong, I. Staude, A. James, J. Dominguez, S. Liu, S. Campione, G. S. Subramania, T. S. Luk, M. Decker, D. N. Neshev, I. Brener, and Y. S. Kivshar, Nano Lett. **15**, 5369 (2015).
25. P. Grahn, A. Shevchenko, and M. Kaivola, New J. Phys. **14** (2012).
26. S. Makarov, S. Kudryashov, I. Mukhin, A. Mozharov, V. Milichko, A. Krasnok, and P. Belov, Nano Lett. **15**, 6187 (2015).
27. T. Lewi, P. P. Iyer, N. A. Butakov, A. A. Mikhailovsky, and J. A. Schuller, Nano Lett. **15**, 8188 (2015).
28. M. R. Shcherbakov, P. P. Vabishchevich, A. S. Shorokhov, K. E. Chong, D. Y. Choi, I. Staude, A. E. Miroshnichenko, D. N. Neshev, A. A. Fedyanin, and Y. S. Kivshar, Nano Lett. **15**, 6985 (2015).

FULL REFERENCES

1. P. Moitra, B. a. Slovick, Z. Gang Yu, S. Krishnamurthy, and J. Valentine, "Experimental demonstration of a broadband all-dielectric metamaterial perfect reflector," Appl. Phys. Lett. **104**, 171102 (2014).
2. S. Liu, M. B. Sinclair, T. S. Mahony, Y. C. Jun, S. Campione, J. Ginn, D. A. Bender, J. R. Wendt, J. F. Ihlefeld, P. G. Clem, J. B. Wright, and I. Brener, "Optical magnetic mirrors without metals," Optica **1**, 250 (2014).
3. P. Moitra, B. A. Slovick, W. Li, I. I. Kravchencko, D. P. Briggs, S. Krishnamurthy, and J. Valentine, "Large-Scale All-Dielectric Metamaterial Perfect Reflectors," ACS Photonics **2**, 692–698 (2015).
4. Z. Ma, S. M. Hanham, P. Albella, B. Ng, H. T. Lu, Y. Gong, S. A. Maier, and M. Hong, "Terahertz All-Dielectric Magnetic Mirror Metasurfaces," ACS Photonics **3**, 1010–1018 (2016).
5. N. K. Grady, J. E. Heyes, D. R. Chowdhury, Y. Zeng, M. T. Reiten, A. K. Azad, A. J. Taylor, D. A. R. Dalvit, and H.-T. Chen, "Terahertz Metamaterials for Linear Polarization Conversion and Anomalous Refraction," Science **340**, 1304–1307 (2013).
6. Y. Ye and S. He, "90° Polarization Rotator Using a Bilayered Chiral Metamaterial With Giant Optical Activity," Appl. Phys. Lett. **96**, 1–4 (2010).
7. J. Hao, Y. Yuan, L. Ran, T. Jiang, J. A. Kong, C. T. Chan, and L. Zhou, "Manipulating electromagnetic wave polarizations by anisotropic metamaterials," Phys. Rev. Lett. **99**, 1–4 (2007).
8. A. Pors, M. G. Nielsen, G. D. Valle, M. Willatzen, O. Albrektsen, and S. I. Bozhevolnyi, "Plasmonic metamaterial wave retarders in reflection by orthogonally oriented detuned electrical dipoles," Opt. Lett. **36**, 1626 (2011).
9. M. Pu, P. Chen, Y. Wang, Z. Zhao, C. Huang, C. Wang, X. Ma, and X. Luo, "Anisotropic meta-mirror for achromatic electromagnetic polarization manipulation," Appl. Phys. Lett. **102** (2013).
10. S. Xiao, H. Mühlenbernd, G. Li, M. Kenney, F. Liu, T. Zentgraf, S. Zhang, and J. Li, "Helicity-Preserving Omnidirectional Plasmonic Mirror," Adv. Opt. Mater. **4**, 654–658 (2016).
11. Q. Zhao, J. Zhou, F. Zhang, and D. Lippens, "Mie resonance-based dielectric metamaterials," Mater. Today **12**, 60–69 (2009).
12. A. Arbabi, Y. Horie, M. Bagheri, and A. Faraon, "Dielectric Metasurfaces for Complete Control of Phase and Polarization with Subwavelength Spatial Resolution and High Transmission," Nat. Nanotechnol. **10**, 937–943 (2014).
13. A. Arbabi, Y. Horie, A. J. Ball, M. Bagheri, and A. Faraon, "Subwavelength-thick Lenses with High Numerical Apertures and Large Efficiency Based on High Contrast Transmitarrays," Nat. Commun. **6**, 7069 (2014).
14. M. P. Backlund, A. Arbabi, P. N. Petrov, E. Arbabi, S. Saurabh, A. Faraon, and W. E. Moerner, "Removing orientation-induced localization biases in single-molecule microscopy using a broadband metasurface mask," Nat. Photonics **10**, 459–462 (2016).
15. S. Kruk, B. Hopkins, I. I. Kravchenko, A. Miroshnichenko, D. N. Neshev, and Y. S. Kivshar, "Broadband highly efficient dielectric metadevices for polarization control," APL Photonics **1**, 030801 (2016).
16. M. Khorasaninejad, W. T. Chen, R. C. Devlin, J. Oh, A. Y. Zhu, and F. Capasso, "Metalenses at visible wavelengths: Diffraction-limited focusing and subwavelength resolution imaging," Science **352**, 1190–1194 (2016).
17. R. Magnusson and M. Shokooh-Saremi, "Physical basis for wideband resonant reflectors." Opt. Express **16**, 3456–3462 (2008).
18. F. Lu, F. G. Sedgwick, V. Karagodsky, C. Chase, and C. J. Chang-Hasnain, "Planar high-numerical-aperture low-loss focusing reflectors and lenses using subwavelength high contrast gratings," Opt. Express **18**, 12606 (2010).
19. C. J. Chang-Hasnain and W. Yang, "High-contrast gratings as new platform for integrated optoelectronics," Adv. Opt. Photonics **4**, 379–440 (2012).
20. Y. Yang, W. Wang, P. Moitra, I. I. Kravchenko, D. P. Briggs, and J. Valentine, "Dielectric Meta-Reflectarray for Broadband Linear Polarization Conversion and Optical Vortex Generation," Nano Lett. **14**, 1394–1399 (2014).
21. M. Decker, I. Staude, M. Falkner, J. Dominguez, D. N. Neshev, I. Brener, T. Pertsch, and Y. S. Kivshar, "High-Efficiency Dielectric Huygens' Surfaces," Adv. Opt. Mater. **3**, 813–820 (2015).
22. J. C. Ginn, I. Brener, D. W. Peters, J. R. Wendt, J. O. Stevens, P. F. Hines, L. I. Basilio, L. K. Warne, J. F. Ihlefeld, P. G. Clem, and M. B. Sinclair, "Realizing Optical Magnetism from Dielectric Metamaterials," Phys. Rev. Lett. **108**, 097402 (2012).
23. I. Staude, A. E. Miroshnichenko, M. Decker, N. T. Fofang, S. Liu, E. Gonzales, J. Dominguez, T. S. Luk, D. N. Neshev, and I. Brener, "Tailoring directional scattering through magnetic and electric resonances in subwavelength silicon nanodisks," ACS Nano **7**, 7824–7832 (2013).
24. K. E. Chong, I. Staude, A. James, J. Dominguez, S. Liu, S. Campione, G. S. Subramania, T. S. Luk, M. Decker, D. N. Neshev, I. Brener, and Y. S. Kivshar, "Polarization-Independent Silicon Metadevices for Efficient Optical Wavefront Control," Nano Lett. **15**, 5369–5374 (2015).
25. P. Grahn, A. Shevchenko, and M. Kaivola, "Electromagnetic multipole theory for optical nanomaterials," New J. Phys. **14** (2012).
26. S. Makarov, S. Kudryashov, I. Mukhin, A. Mozharov, V. Milichko, A. Krasnok, and P. Belov, "Tuning of Magnetic Optical Response in a Dielectric Nanoparticle by Ultrafast Photoexcitation of Dense Electron-Hole Plasma," Nano Lett. **15**, 6187–6192 (2015).
27. T. Lewi, P. P. Iyer, N. A. Butakov, A. A. Mikhailovsky, and J. A. Schuller, "Widely Tunable Infrared Antennas Using Free Carrier Refraction," Nano Lett. **15**, 8188–8193 (2015).
28. M. R. Shcherbakov, P. P. Vabishchevich, A. S. Shorokhov, K. E. Chong, D. Y. Choi, I. Staude, A. E. Miroshnichenko, D. N. Neshev, A. A. Fedyanin, and Y. S. Kivshar, "Ultrafast All-Optical Switching with Magnetic Resonances in Nonlinear Dielectric Nanostructures," Nano Lett. **15**, 6985–6990 (2015).